CrossMark

Computational Homogenization of Mechanical Properties for Laminate Composites Reinforced with Thin Film Made of Carbon Nanotubes

A. El Moumen [1] · M. Tarfaoui [1] · K. Lafdi [2]

Abstract Elastic properties of laminate composites based Carbone Nanotubes (CNTs), used in military applications, were estimated using homogenization techniques and compared to the experimental data. The composite consists of three phases: T300 6k carbon fibers fabric with 5HS (satin) weave, baseline pure Epoxy matrix and CNTs added with 0.5%, 1%, 2% and 4%. Two step homogenization methods based RVE model were employed. The objective of this paper is to determine the elastic properties of structure starting from the knowledge of those of constituents (CNTs, Epoxy and carbon fibers fabric). It is assumed that the composites have a geometric periodicity and the homogenization model can be represented by a representative volume element (RVE). For multi-scale analysis, finite element modeling of unit cell based two step homogenization method is used. The first step gives the properties of thin film made of epoxy and CNTs and the second is used for homogenization of laminate composite. The fabric unit cell is chosen using a set of microscopic observation and then identified by its ability to enclose the characteristic periodic repeat in the fabric weave. The unit cell model of 5-Harness satin weave fabric textile composite is identified for numerical approach and their dimensions are chosen based on some microstructural measurements. Finally, a good comparison was obtained between the predicted elastic properties using numerical homogenization approach and the obtained experimental data with experimental tests.

Keywords Homogenization · Computational multi-scale modeling · Composite materials · Carbon nanotubes · Micromechanical modelling · Textile composites

✉ A. El Moumen
ahmed.el_moumen@ensta-bretagne.fr

[1] ENSTA Bretagne, FRE CNRS 3744, IRDL, F-29200 Brest, France

[2] University of Dayton, Dayton, OH 45469-0168, USA

🖄 Springer

1 Introduction

Composites reinforced with nano-additives such as carbon nanotubes (CNTs) and nanoclays have become a subject of numerous research projects, Lafdi and Matzek [1] and Song and Youn [2]. The determination of the mechanical behavior of CNTs reinforced composites has attracted a large attention, because the excellent properties of CNTs, Bhushan [3], Després et al. [4], Falvo et al. [5], Lau et al. [6] and Li et al. [7]. A wide variety of composites containing CNTs have been identified for various applications. CNTs added to ceramics, polymers and metallic matrix were studied by Brune and Bicerano [8], Kwon et al. [9] and Peigney et al. [10], respectively. A review papers were published on this subject, Bakshi et al. [11], Coleman et al. [12] and Thostenson et al. [13]. To assess the potential and properties of these new nanocomposites three approaches were used: experimental, analytical and numerical simulation.

Experimental investigations on mechanical properties of the composite based CNTs have shown an improvement of properties compared to those of the matrix only, Schadler et al. [14], Zhu et al. [15] and Tarfaoui et al. [16]. Analytical studies were based on the theory of bounds or models, Buryachenko [17], and numerical methods involved more finite element method or molecular dynamic simulations, Cao and Chen [18]. El Moumen et al. [19] give a list of some micromechanical models used for modeling of composite materials and extended by Djebara et al. [20] for polymer nanocomposites. These authors show that in the case of minor volume fractions (<5%), the analytical models, excluding mixture lows, give the same results compared to experimental data and numerical predictions. The considered models are: Voigt-Reuss and Hashin-Shtrikman bounds, Hashin and Shtrikman [21], Mori-Tanaka model, Mori and Tanaka [22], generalized self consistent (GSC) estimates of Christensen and Lo [23] and Halpin-Tsai model, see Halpin and Kardos [24]. In a series of papers, Odegard et al. [25], Odegard et al. [26], Odegard et al. [27] and Odegard et al. [28] have modeled analytically the composite materials reinforced by CNTs using the equivalent continuum method and the Mori–Tanaka micromechanics method to obtain the elastic moduli. Generally, for CNT composites, Halpin-Tsai equation and Mori-Tanaka model are widely used. In another investigation, Yeh et al. [29], Halpin-Tsai equation was used to estimate the elastic modulus of polymers containing CNTs. It should be mentioned that analytical models depend on the CNTs distributions. For example, aligned CNTs are modeled with Halpin-Tsai equation or Hashin and Rosen [30] approach and Mori-Tanaka or GSC models for Non-aligned CNTs (random particles). The analytical models and their accuracy based on suitable hypotheses do not give correct and exact solution, especially in the case of important volume fractions and/or high Young's modulus (case of CNT). The best solution can only be obtained by solving numerically the boundary value problem.

Numerical simulation of the mechanical properties of composites containing CNTs is a novel technique for designing composites with complex morphologies. This approach is divided into two methods depending on the scale analysis: molecular dynamics simulation and continuum mechanics. Chen and Liu [31] have simulated numerically the effective elastic properties of composites embedded with CNTs using finite element method based on the representative volume element (RVE) notion. The authors show that there are good agreements between estimated numerical results compared to experimental ones. Others studies focus on the prediction of physical properties by using homogenization method, Deng et al. [32], El Moumen et al. [33], El Moumen et al. [34], Ioannou et al. [35], Kaddouri et al. [36], Seidel and Lagoudas [37], Terada et al. [38], and Pagano and Yuan [39]. The homogenization method, based FEM, is a powerful technique by which a heterogeneous medium is transformed to the equivalent homogeneous medium, Manta et al. [40]. Selmi et al. [41] have introduced the

homogenization techniques to estimate the effective properties of single walled carbon nanotube reinforced polymers. The effect of CNTs on effective elastic properties of composite materials have been studied by Fisher et al. [42] and Fisher et al. [43] using numerical simulation techniques based finite elements coupled with Mori-Tanaka model. A numerical investigation for the calculation of elastic constants of nanocomposites containing CNTs was proposed by Buryachenko [17].

Recently, Ren et al. [44] present a 3D numerical computational modeling of polymer composites reinforced by CNTs. The multi-scale numerical model is represented by a hexagonal RVE for the CNT polymer and the simulation is conducted by homogenization technique with FE method. A computational procedure based RVE was proposed by Savvas et al. [45] for the determination of physical properties of CNTs reinforced composites. Computational homogenization was applied on various RVE finite element models using both of kinematic and static uniform boundary conditions. The presented numerical results demonstrate that the effect of CNT waviness is minimal, while CNT orientation has the dominant effect. Gupta and Harsha [46] have studied the mechanical properties of CNTs reinforced polymer composites using multi-scale finite element approach. These composite materials consist of aligned CNTs that are uniformly distributed within the polymer matrix. The multi-scale finite element model was developed by Choi et al. [47] and Zhou et al. [48] for the identification of mechanical properties of single-walled CNTs reinforced polymer nano-composites.

In this work, we develop several micromechanical models to estimate elastic moduli of textile composites reinforced with CNTs. First, a numerical model based on microscope measurements and TexGen software is considered. Second, a multi-scale approach based finite element method (FEM) is used, which allows to model fully non-aligned dispersed CNTs in textile composites. Third, a comparison between results of numerical models and experimental data is presented.
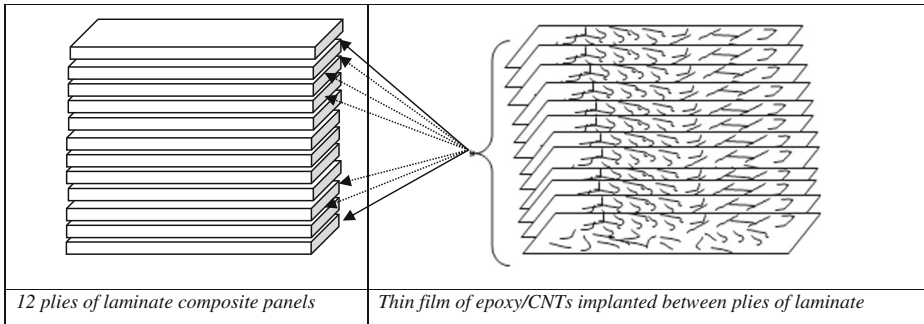
2 Materials and Manufacturing Process

The materials used in this study were epoxy matrix, T300 6 k carbon fibers fabric with 5 Harness Satin (HS) architecture provided by Hexell Company and CNTs provided by Nanocyl Belgium Company. The nanotubes have an average diameter of the order of 10 nm and length of 1.5 μm. Morphology shows that the CNTs are observed as long curved cylindrical fibers with snake-like shape.

The methodology employed in this investigation for manufacturing process of laminate composites with thin film made of CNTs is presented in Fig. 1. It consists to implant thin layers of nanotubes onto the surfaces of 5-HS fabric. First, nanocomposite film was manufactured. For that purpose, CNTs were mixed with Epoxy resin using a high shear laboratory mixer at 2000 rpm for 30 min and the film with 120 μm in thickness is manufactured using film line, Fig. 2a. This film is used as interleave between carbon fabrics, Fig. 2b. For more illustration concerning material properties, microstructures and manufacturing process see our previous works, see El Moumen et al. [49] and El Moumen et al. [50].

3 3D Computational Multi-Scale Model of CNT Based Composites

3D computational multi-scale numerical model is proposed to estimate the elastic properties of such composites. The multi-scale approach is able to estimate macroscopic properties via those

| 12 plies of laminate composite panels | Thin film of epoxy/CNTs implanted between plies of laminate |

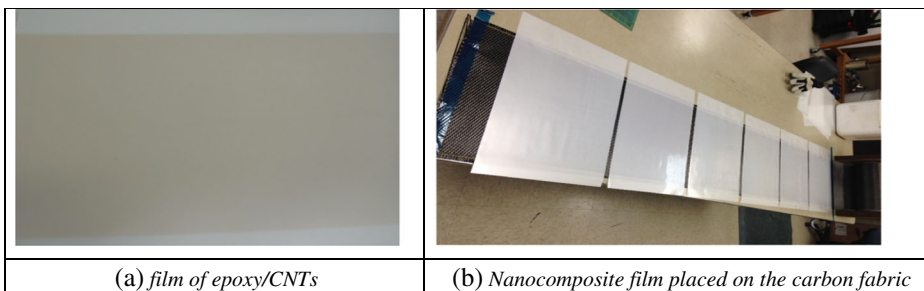**Fig. 1** Schematic representation of manufacturing process

of constituents (Epoxy, Carbon fabric and CNTs) and architecture of composites. The effective elastic properties are homogenized by using finite element method based two step homogenization techniques and representative volume element (RVE).

### 3.1 Schematic Presentation of the Multi-Scale Model

The multi-scale architecture of the textile composites is more complex. It consists of three phases: Epoxy matrix, CNTs randomly distributed and 5-Harness satin weave fabric. Actually there is no FE software can model directly this type of geometries. The idea consists of using two step homogenization techniques. This technique aims to reduce 3-phase materials into 2-phase where all FE codes can model.

The principle of the two-step homogenization used in this section is depicted on Fig. 3 for textile composites with random CNTs. Firstly, the matrix and CNTs phase are actually treated as a separate composite phase. Epoxy resin reinforced with a random distribution of small CNTs volume fractions constitutes a simple composite material, named here composite 1 (or pseudo domain 1). Then, the three phase composites is virtually reduced into a two phase: composite 1 "Epoxy and CNTs" and composite 2 "carbon fibers fabric". Secondly, the homogenized effective properties of composite 1 were used as input data in the second step homogenization.

Two-phase pseudo domain, or composite 1, is homogenized (first step) and then the effective elastic properties of the total textile composite are computed by second step. For the composite 1 analytical models and numerical RVE can give the elastic moduli. In this study, we have chosen the GSC models adapted to cylindrical fibers compared with numerical

| (a) *film of epoxy/CNTs* | (b) *Nanocomposite film placed on the carbon fabric* |

Fig. 2 Manufacturing process
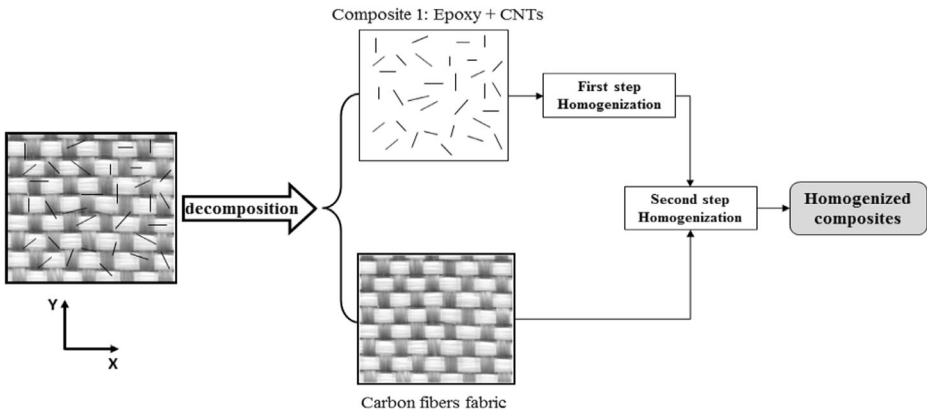
Fig. 3 Schematic representation of two-step homogenization techniques for the effective elastic properties of laminate composites containing CNTs

results, because their abilities to homogenize such composites (Epoxy with random CNTs). These models give the same results in the case of low cylindrical fibers volume fractions, El Moumen et al. [19]. Therefore, for different fractions considered in this study (0.5%, 1%, 2% and 4%), GSC and numerical RVE are used to estimate the effective elastic properties of CNTs/Epoxy.

A way to achieve the homogenization of textile composite is to use the obtained results by first step homogenization as input data, which play a role of the matrix reinforced with carbon fibers fabric in the second step, Fig. 1.

3.2 Effective Properties and Behavior of Phases

The carbon fibers used in the present study are considered as orthotropic behavior, whose longitudinal direction which is defined by 11 and the transverse plan is defined by 22 and 33 directions. The six elastic moduli of the carbon fibers used for multi-scale modeling are given in Table 1. The Epoxy matrix and CNTs are assumed to be isotropic. Their elastic moduli are also given in Table 1.

The orthotropic behavior of the yarns can be defined by a 3D stiffness matrix consisting of nine independent constants as shown in Eq. 1. Incorporating transversely isotropic yarn behavior, the final stiffness matrix consists of the five independent constants. We recall that the used homogenization technique consists of reducing the three phase composite to two phase: phase 1 "Epoxy + CNTs" and phase 2 "carbon fibers fabric". Therefore, the homogenized effective elastic properties, with numerical and analytical models, of Epoxy matrix reinforced with CNTs are listed in Table 2 for different volume fractions. It should be

Table 1 Elastic moduli of carbon fiber, Epoxy matrix and CNTs

	E_{11} (GPa)	$E_{22} = E_{33}$ (GPa)	G_{12} (GPa)	G_{13} (GPa)	G_{23} (GPa)	ν_{12}	ν_{13}	ν_{23}
Carbon fibers	230	15	15	15	15	0.2	0.2	0.2
	E (GPa)			ν (GPa)				
Epoxy matrix	2.72			0.3				
CNTs	500			0.26				

Table 2 Homogenized effective elastic moduli of CNTs/Epoxy

		0%	0.5%	1%	2%	4%
Numerical RVE	E (GPa)	2.72	2.75	2.80	2.9	3.06
	ν	0.3	0.3	0.29	0.29	0.29
Analytical model	E (GPa)	2.72	2.74	2.76	2.80	2.88
	ν	0.3	0.3	0.29	0.29	0.29

mentioned that the generalized self-consistent model and numerical simulation based RVE are used because their capacity to estimate the effective moduli at low volume fractions of cylindrical fibers reinforced matrix. Figure 4a show an example of CNTs/Epoxy RVE used for first step homogenization of elastic moduli. The concentration of stress is observed in CNTs/Matrix interphase region. Nano-scale RVE of Epoxy/CNTs showed the fiber shape and presented in Fig. 4b. It appears that the nanotubes have a tendency to cluster and create the agglomerations.

$$
S_{ij} = \begin{pmatrix}
\dfrac{1}{E11} & \dfrac{-\nu_{12}}{E11} & \dfrac{-\nu_{13}}{E11} & 0 & 0 & 0 \\[2mm]
\dfrac{-\nu_{12}}{E11} & \dfrac{1}{E22} & \dfrac{-\nu_{23}}{E22} & 0 & 0 & 0 \\[2mm]
\dfrac{-\nu_{13}}{E33} & \dfrac{-\nu_{23}}{E33} & \dfrac{1}{E33} & 0 & 0 & 0 \\[2mm]
0 & 0 & 0 & \dfrac{1}{G23} & 0 & 0 \\[2mm]
0 & 0 & 0 & 0 & \dfrac{1}{G13} & 0 \\[2mm]
0 & 0 & 0 & 0 & 0 & \dfrac{1}{G12}
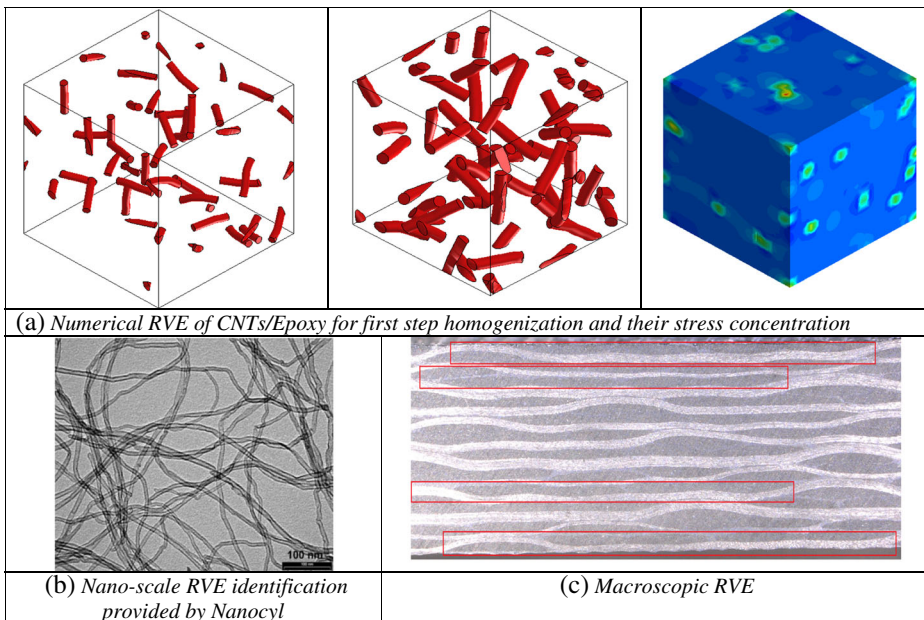\end{pmatrix}
\tag{1}
$$

3.3 Geometric Parameters of Investigated Textile

The first step of our methodology consists of identifying geometrically the RVE composite by using a KAYENCE microscope. Figure 4c gives an example of the textile composite image obtained by microscope. According to the periodicity characteristic of the composite, the identified macroscopic RVEs are shown in the image with red rectangles.

To construct a total unit cell of geometric model, a series of microscopic observations are considered. These observations allow to measure global characteristics of the RVE as: length, width, thickness, weft yarn, gap between yarns, yarn thickness, fabric thickness, fiber section, etc. The geometrical measured variables for the textile RVE are illustrated in Fig. 5a. An example of the microscopic images regrouping experimental measurements is depicted on Fig. 5b and their average value is tabulated in Table 3. Finally, all the experimental measurements are used to construct a RVE used for homogenization of the elastic moduli of textile composite with CNTs.

3.4 Geometric Model of Investigated Textile

Using measured parameters for the weave textile composite RVE presented in Table 3, the geometric weave textile is modeled by TexGen software, Sherburn and Long [51]. The carbon

(a) *Numerical RVE of CNTs/Epoxy for first step homogenization and their stress concentration*

(b) *Nano-scale RVE identification provided by Nanocyl*

(c) *Macroscopic RVE*

**Fig. 4** Identification of RVE model in specimens

fibers fabric is characterized by the interlacement of the warp and weft carbon yarns, resulting in undulation in both directions. Generally, the volume of yarn is not entirely occupied by carbon fibers because the flow of epoxy between micro-fibrils. However, for modeled RVE, fibers constitute a yarn are not modeled individually, but the yarns are considered as a solid volume because this representation is more practical for the computation time and CPU processor speed and memory, Sherburn [52]. An example of the RVE based experimental measurements using TexGen is presented on Fig. 6a and compared to real RVE of Fig. 6b.

3.5 Mesh of RVE Composites

TexGen and ABAQUS software are used in combination to mesh RVE of textiles because of their similarity and ability to enable the creating of textile models, Dixit et al. [53]. The geometric model generated by the TexGen software is first exported into ABAQUS Voxel File environment, and then saved in the form of. Inp file with complete textile (matrix and fibers) and meshing data. Issues related to FE modeling such as contact between the yarns are taken care of by the ABAQUS and TexGen softwares. According to Dixit et al. [53], three dimensions 8 nodded brick element with reduced integration (C3D8R) were found to be the most applicable element for these types of composites. Thus, element types of C3D8R are used in this study. However, the inter-face between the micro-fibrils and matrix is not considered in this study because the micro–structure constituted of the microfibers and the matrix and also the needed memory to mesh the inter-face region. Moreover, this is considered to reduce the computational time and cost, because the interface region can increase dramatically the cost and time computational. Therefore the perfect contact is considered. For illustration, an example
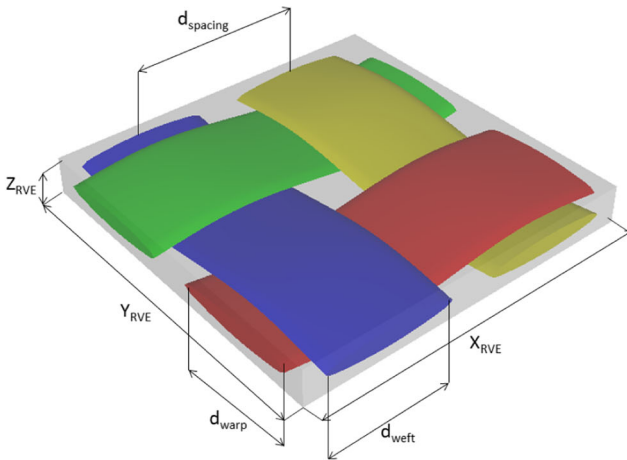
(a) *Geometrical parameters of the RVE as given in table 3.*
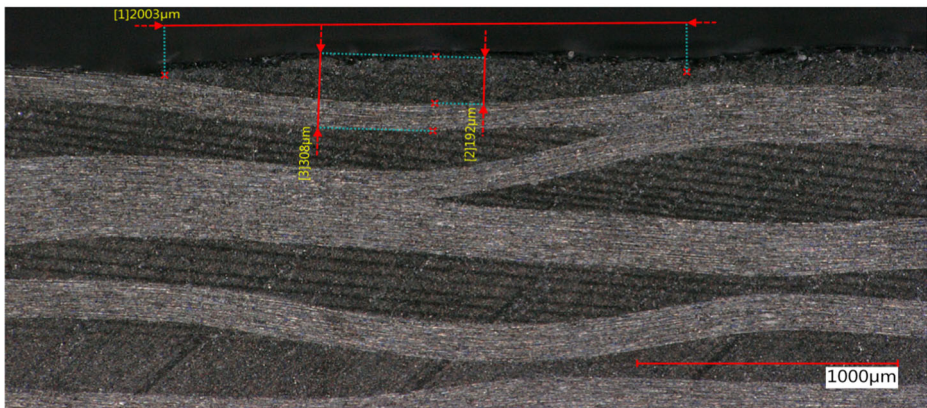
(b) *Experimental measurements of some RVE geometric parameters.*

Fig. 5 Geometrical parameters of the RVE as given in Table 3

of the carbon fibers fabric mesh and matrix proposed for numerical simulations is presented on Fig. 7. This mesh contains more than 80,000 elements.

Finally, the generated and meshed RVEs by TexGen and ABAQUS softwares are exported to ZeBulon software for numerical homogenization. Both yarns and matrix volumes are exported to Zebulon forma.

Table 3 Parameterization for the weave textile composite RVE displayed in Fig. 5. All values are shown in mm unit

	X_{RVE}	Y_{RVE}	Z_{RVE}	d_{Weft}	d_{Warp}	$d_{spacing}$
Measure 1	10.7	10.7	0.34	2	2	2.2
Measure 2	9.1	9.1	0.3	1.40	1.40	1.42
Measure 3	7	7	0.32	1.30	1.30	1.32
Average value	8.9	8.9	0.32	1.5	1.5	1.6

(a) *Simulated model based on experimental measures*

(b) *Real RVE*
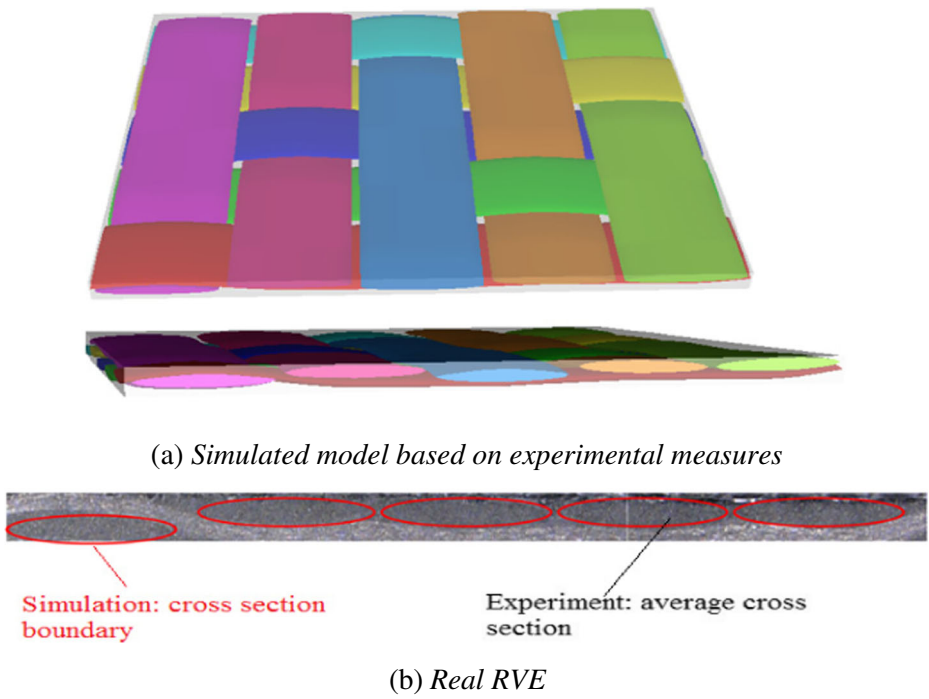
Fig. 6 Geometric model for 5-Harness satin weave fabric

(a) *Carbon fibers*
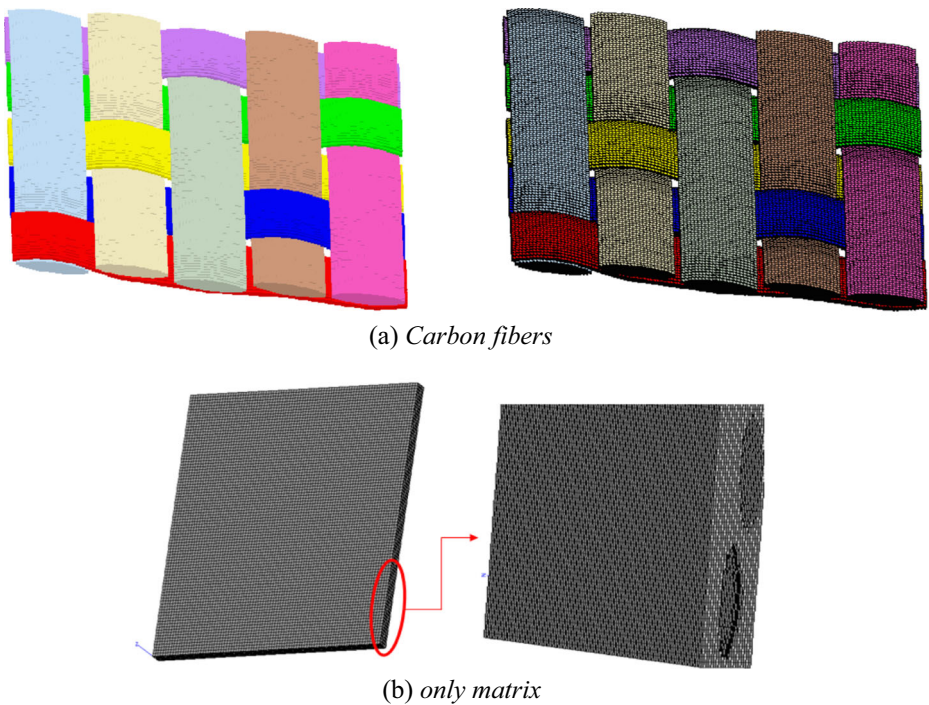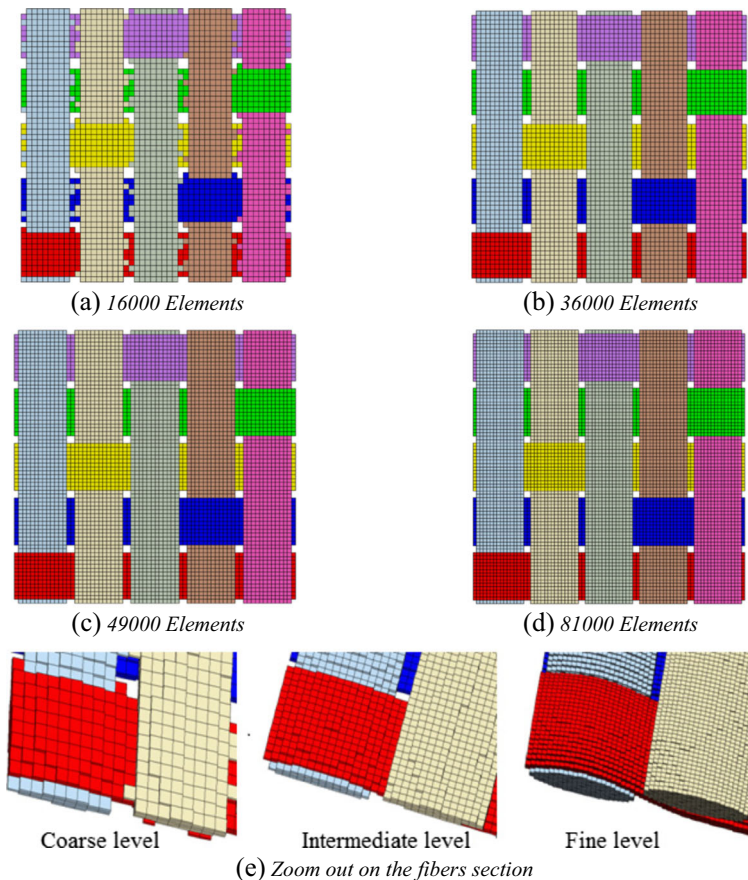

(b) *only matrix*

Fig. 7 Textile composite RVE meshes: **a** carbon fibers fabric and **b** only matrix

3.6 Numerical Homogenization

The objective of this section is to estimate numerically the effective elastic moduli of textile composites containing different fraction of CNTs. These moduli are: E_{11}, E_{22}, E_{33}, G_{12}, G_{13}, G_{23}, ν_{12}, ν_{13} and ν_{23}. The finite element model is based on morphological data obtained from physical characterization of specimens using microscope. Numerical homogenizations need an optimization of meshes (a mesh convergence study). Then, the mesh density is firstly studied.

3.6.1 Mesh Density and Convergence of Elastic Moduli

The mesh density is defined by Kanit et al. [54] and El Moumen et al. [55] as the minimum number of elements necessary to mesh the composite volume. In this part we investigate at what level of mesh refinement, the convergence of elastic moduli can be expected for typical textile composites. For that purpose, four RVEs levels of mesh refinement are created in terms of the accuracy of results and computational time. Figure 8 gives the different mesh resolutions used to study the convergence. The number of nodes ranging from 28,617 (coarse level), for a mesh containing 16,000 EFs and 55,473 DOF, to 72,177 nodes (fine level), for a mesh

(a) *16000 Elements*

(b) *36000 Elements*

(c) *49000 Elements*

(d) *81000 Elements*

Coarse level   Intermediate level   Fine level

(e) *Zoom out on the fibers section*

Fig. 8 Example of RVE meshes

containing 81,000 EFs. For illustration, a zoom out on the elliptical fibers section is also presented on this figure for three number of FE. It appears that the fine level corresponds to real fibers section.

The variation of the elastic shear modulus as a function of the FE number is studied. Figure 9 shows that the elastic moduli of the composite first rapidly decrease for finer mesh, or coarse level, and tend to be stabilized in the case of high mesh resolutions. This figure shows also that the mesh density of level 4 is sufficient to provide the acceptable convergence of numerical results. For more accurate of results, the mesh density of level 6 is considered in this study. Hence, further numerical computational are performed using a mesh density level 6 which containing 81,000 elements.

3.6.2 Modeling Results and Discussions

In this section, the numerical results are performed using the FE model developed in the previous section. The mechanical behaviors of the RVE under loading in three directions are characterized. In order to obtain nine elastic moduli of textile composites with CNTs, two types of tests are considered in this study: tension and shear tests. There are six loads cases and the output results give the orthotropic elastic behavior of composite textile (E_{11}, E_{22}, E_{33}, G_{12}, G_{13}, G_{23}, ν_{12}, ν_{13} and ν_{23}). The principle consists in determining the macroscopic elastic moduli of the textile from the properties of its constituents. For this, a first process homogenized the Epoxy matrix and CNTs and the second process determines the properties of the entire composite. RVE model consists of two phases: matrix phase with elastic properties listed in Table 1 and the fabric phase of carbon fibers with isotropic transverse behavior listed in the same table. Computations are performed using the hypothesis of small deformation; therefore the volume variation is quietly small. The effect of volume fraction is numerically studied. The axial and transverse effective moduli for composites with CNTs are given versus volume fraction in Tables 4, 5 and 6. As can be seen, numerical results shows that the added of minor amount of CNTs in the matrix affect the composite textile moduli, especially for Z-direction properties. It appears that the elastic moduli increase with increasing CNTs amount. It should be mentioned that the mechanical behavior of the RVE under tensile strain is fiber dominated. However, in the case of shear test is matrix dominated, and the influence of the fibers architecture becomes less. The relationship $\nu_{12}/E_{11}=\nu_{21}/E_{22}$ is verified.
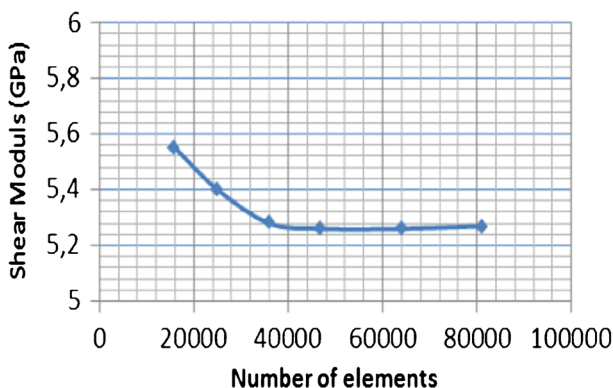
Fig. 9 Variation of the elastic moduli vs. number of elements

Table 4 Predicted Young's moduli versus volume fraction of CNTs

	0%	0.5%	1%	2%	4%
E_{11} (GPa)	59.11	59.138	59.16	59.219	59.33
E_{22} (GPa)	59	59	59	59	58.55
E_{33} (GPa)	7.6	7.623	7.6	7.67	7.81

The multi-scale computations based tension and shear tests provides also access to local properties as principle stress σ_{11}. Figures 10 and 11 present the local distribution of the stress for tension and shear tests, respectively, when a deformation is applied in the fiber direction. It appears that the stresses are localized at interweaving region and near the edge of the matrix/fabric interface, Fig. 10. Indeed, the interweaving represents the most rigid phase of the textile composites. Moreover, a heterogeneous distribution of stress is observed within fibers. These can be considered as region for the initiation of damage and [56] showed that damage propagates and initiates at similar regions. From these remarks, damage and delamination phenomenon may be instantaneously propagates into the fibers and the matrix/fibers interfaces. Figure 12 illustrates an example of examined samples with observed damage. This figure validates the numerical results of Figs. 10 and 11 which state that the damage and cracks appear at interweaving zone (site of stress localization).

4 Confrontation of Numerical Results with Experimental Data

To validate the homogenized elastic moduli presented in the previous section, these are used to simulate macroscopic experimental tests at different volume fractions of CNTs. Experimental tests provide a typical stress strain, or load-displacement, curves. A FE model was established with ABAQUS software, and applied in the case of Open Hole tension (OHT) test and Short Beam Shear (SBS) test. Experimental characterization and methodology of manufacturing process were given in our previous works, El Moumen et al. [49], El Moumen et al. [50] Tarfaoui et al. [16] and Tarfaoui et al. [57]. The numerical results presented in Tables 4, 5 and 6 are used as input file in the macroscopic FE models. Numerical specimens are generated with the same dimensions of ASTM experimental samples.

4.1 Confrontation in the Case of OHT Test

In this section several cases are discussed for which numerical homogenization results are confronted to experimental data. The cases include OHT test, permits to validate the Young's moduli E11 and E22 and the Poisson ratio. Simulated macroscopic sample is presented on Fig.

**Table 5** Predicted Poisson ratio versus volume fraction of CNTs

	0%	0.5%	1%	2%	4%
ν_{12}	0.089	0.089	0.0892	0.0892	0.0892
ν_{13}	0.27	0.27	0.27	0.274	0.275
ν_{23}	0.28	0.28	0.277	0.279	0.28

**Table 6** Predicted shear moduli versus volume fraction of CNTs

	0%	0.5%	1%	2%	4%
G_{12} (GPa)	8.25	8.257	8.27	8.285	8.316
G_{23} (GPa)	3.97	3.99	4.017	4.04	4.105
G_{13} (GPa)	0.27	0.27	0.27	0.274	0.275

13. The associated mesh for the created macroscopic model is also given in Fig. 13. The three-dimensional solid element C3D8R was used. Because stress was concentrated near the circular notch, the mesh was refined in this zone El Moumen et al. [58].

Figure 14 shows a comparison of the mechanical response of the finite element model to the experimental response for several considered volume fractions. Good correlation is obtained for the majority of the studied cases. These allow validating the obtained elastic moduli using two steps homogenization techniques in section 3. There is a good correlation in elastic region and no damage criteria are considered. The curves deviate beyond the elastic limit where the material starts to be damaged. Therefore, based on OHT results, the estimated Young's moduli and Poisson ratio using homogenization methods represent the elastic behavior of total composites with CNTs. An example of the stress localization in the case of OHT is presented on Fig. 15. This figure shows that the concentration of stress is around the notched zone and can be considered this region as the site of the damage and cracks initiations.
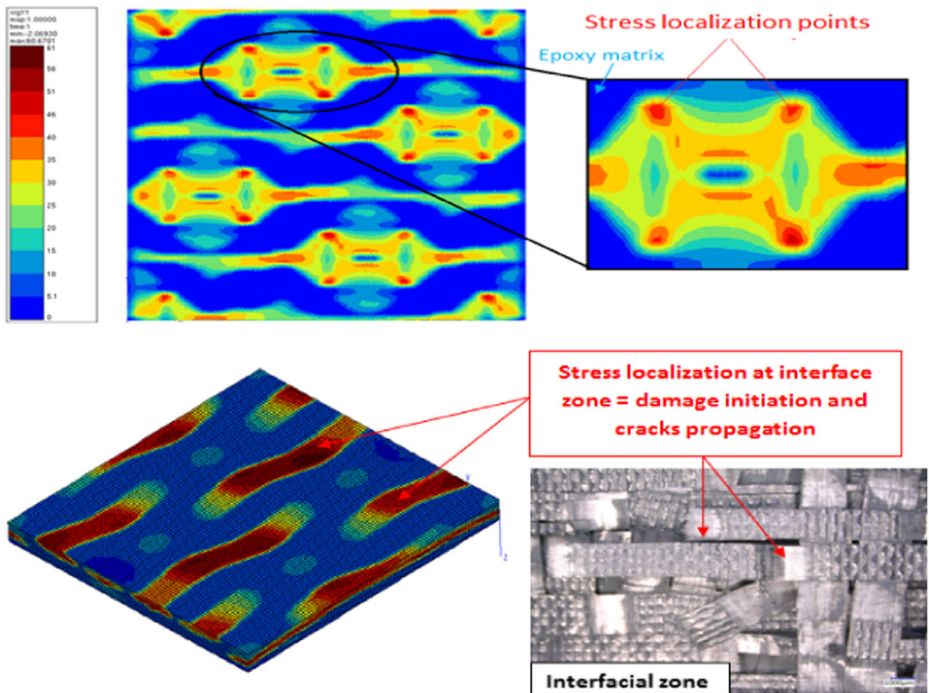
Fig. 10 Stress localization for tension test. The sites stress localization are interweaving zone or fiber/matrix interface which are considered as damage initiation zones
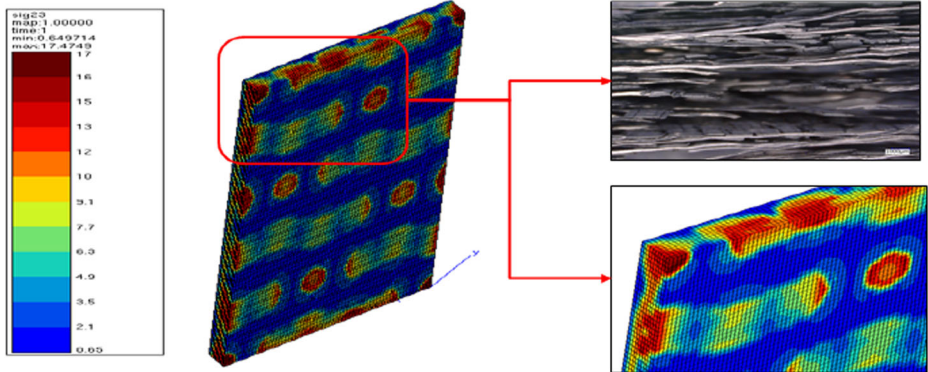
Fig. 11 Example of shear-stress distribution under shear test. At stress localization site, the microscope observation shows that damage and cracks are appeared

4.2 Confrontation in the Case of Short Beam Shear Test (SBS)

In case of shear test, experimental data and numerical results are also confronted and discussed. This test permits to validate the In-plane Young's modulus and the shear moduli. Numerical model and its associate mesh are generated according to ASTM D2344 and presented on Fig. 16 for 3D case.

Figure 17 shows a comparison of the typical graphs load-displacement of numerical models compared to experimental data. A good agreement is observed between results. However, on can deduce that the shear moduli and the In-plane moduli estimated using homogenization techniques in the section 3 can be considered as the mechanical behavior of the structure. Stress distribution in the case of SBS test is given in the Fig. 16d. It appears that the stress concentration is around of indenter zone, which means that this zone can be considered as the damage initiation site.

5 Conclusions and Implications

In this paper, a numerical multi-scale model to simulate the macroscopic elastic moduli of CNT reinforced laminate composites was proposed and compared to the experimental studies.
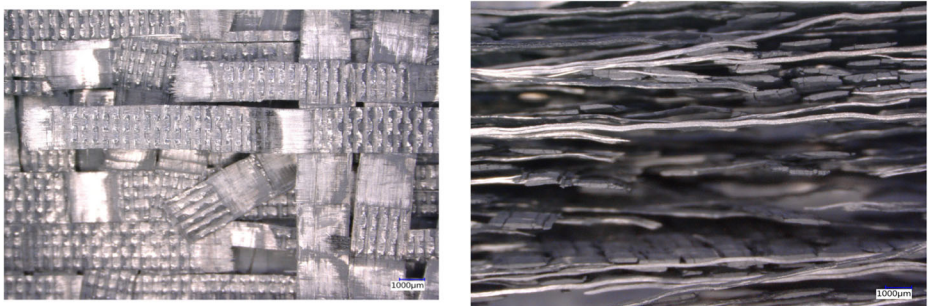

Fig. 12 Zoom out on the damage zone of samples after mechanical tests. The damage appears at interweaving zone and propagates into the fibers directions
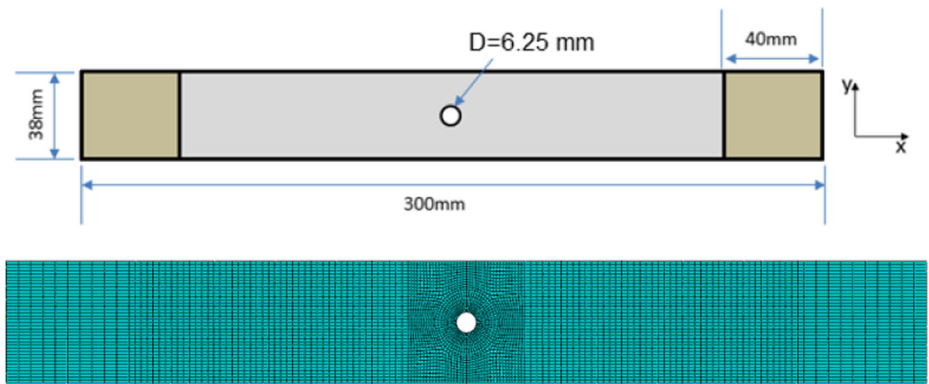
Fig. 13 Macroscopic geometry of Open Hole Tension test for numerical simulation

The micromechanics approaches have been combined through the homogenization methods. The investigated composite consists of three phase materials textile as: Epoxy resin, carbon fibers fabric and CNTs randomly distributed in the matrix. Herein a two-step series of the homogenization technique is used to reduce the three phase materials into two phase case. The generalized self-consistent model and the numerical model at nanoscale are used for first step homogenization, in order to estimate the elastic moduli of Epoxy-CNTs, and then the found results are considered as input data in second step homogenization. The FE method based on the notion of the RVE is chosen for numerical simulation. A RVE of 5 Harness satin fabric
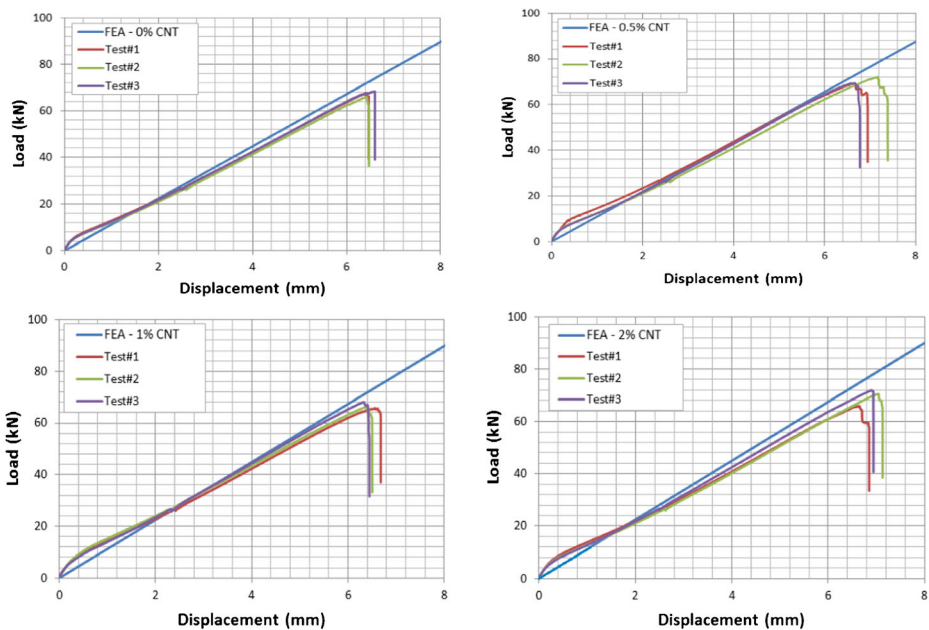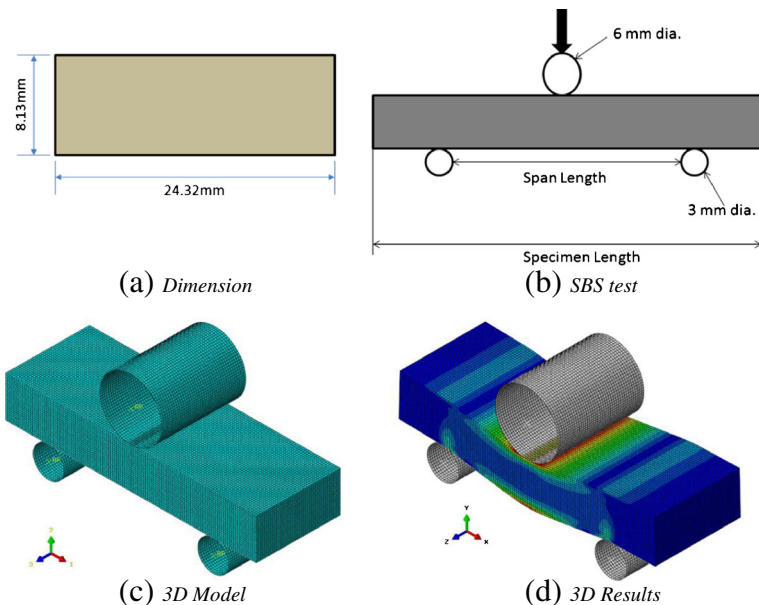

Fig. 14 Confrontation of numerical and experimental results for OHT test. A good tendency in results is obtained
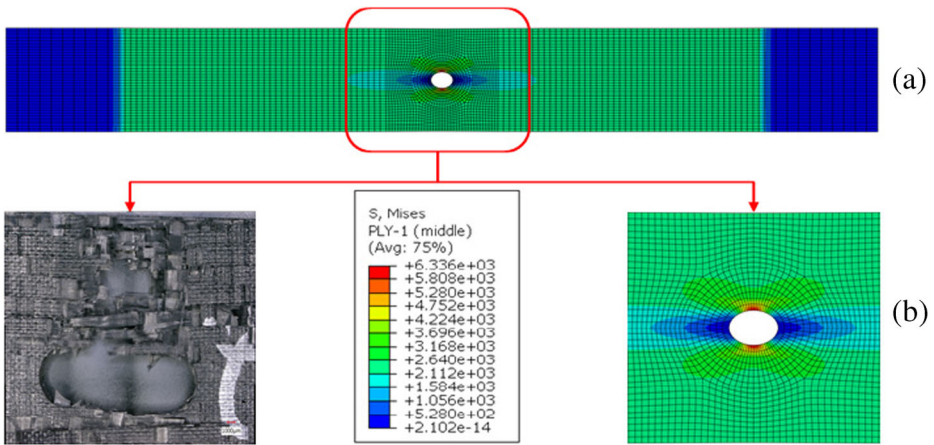
Fig. 15 **a** Stress localization in the case of Open Hole Tension and **b** Zoom out on the notched zone for experimental and numerical tests

composite is performed using a series of microscopic observations with the help of TexGen software. The RVE volume matrix is loaded by a minor amount of CNTs ranging from 0.5% to 4%. However, in order to validate the proposed multi-scale model, the numerical results are compared to the experimental data. The predicted load-displacement curves for various fractions show a good agreement with experimental data. It appears that adding CNTs to traditional polymer composites affect their mechanical properties, especially E_{33} and G_{23}. Mechanical properties of composites change with changing CNTs fraction. Indeed, access to local strain and stress in the RVE was made possible by mapping of local properties. Access to

(a) *Dimension*   (b) *SBS test*

(c) *3D Model*   (d) *3D Results*

Fig. 16 Numerical models and its associate meshes for SBS tests
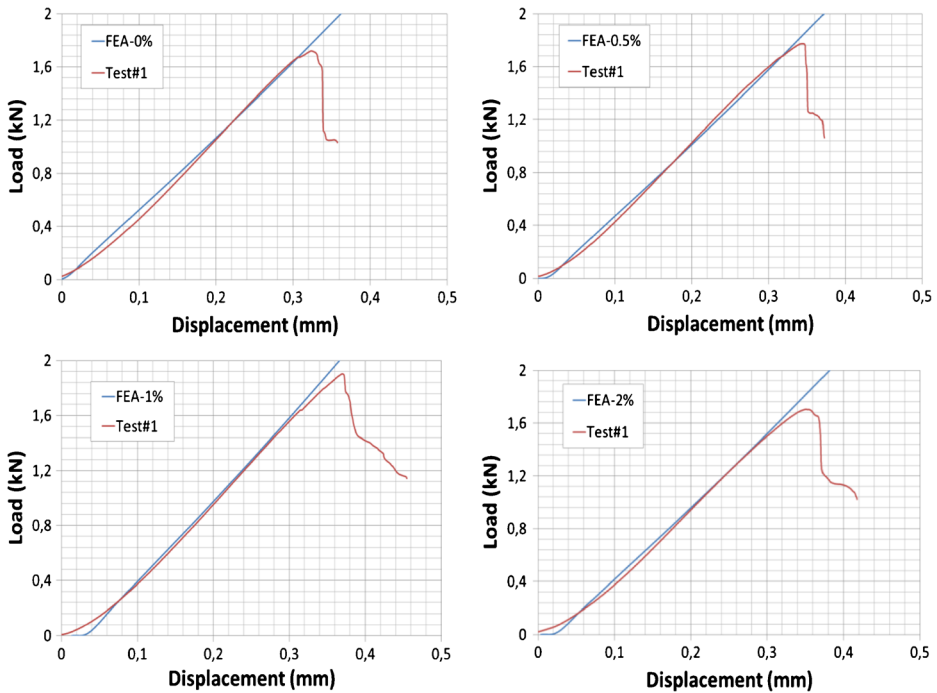
Fig. 17 Confrontation of numerical and experimental results for SBS test at different volume fractions of CNTs

these local fields gives the mechanisms leading to damage composite. It appears that the stress fields are localized at interweaving regions of the textile with CNTs and the strong heterogeneity of the stress distribution is observed for various CNTs fractions. These phenomenons are used to consider the interweaving zone as the principle element to initiate the damage of the composites containing CNTs.

Finally, the numerical model predicts fairly well the Young's moduli E_{11}, E_{22} and E_{33}, the shear modulus G_{12}, Poisson's ratios ν_{12}, ν_{13} and ν_{23}. Moreover, there was an under-estimation of G_{13} and G_{23} shear modulus because de specimens thickness. A small difference is observed in few cases, especially for high volume fractions of CNTs. This difference between the numerical macro-scale and macroscopic experimental data is due to these reasons:

- in the numerical models, the RVE dimensions are generated with a standard deviation,
- both of behavior constituents in the numerical model were assumed to be linear while the Epoxy matrix behavior for example is visco-elastic,
- experimental manufacturing process can affect the elastic moduli,
- CNTs distribution is considered randomly in the homogenization models and some of them can be take aligned distribution,
- mesh resolution can also affect the properties and generates small error, etc.
- distribution of CNTs into nano-scale RVE differ from the experimental specimens.

References

1. Lafdi, K., Matzek, M.: Carbon nanofibers as a nano-reinforcement for polymeric nanocomposites. In: The 35th international SAMPE technical conference at Dayton University, Dayton, Ohio (2003)
2. Song, Y.S., & Youn, J.R.: Modeling of effective elastic properties for polymer based carbon nanotube composites. Polym. **47**(5), 1741–1748 (2006)
3. Bhushan, B.: Springer Handbook of Nano-Technology. Springer, New York (2004)
4. Després, J.F., Daguerre, E., Lafdi, K.: Flexibility of graphene layers in carbon nanotubes. Carbon. **33**, 87–92 (1995)
5. Falvo, M.R., Clary, G.J., Taylor, R.M., Chi, V., Brooks Jr., F.P., Washburn, S., Superfine, R.: Bending and buckling of carbon nanotubes under large strain. Nature (London). **389**, 582–584 (1997)
6. Lau, K.T., Chipara, M., Ling, H.Y., Hui, D.: On the effective elastic moduli of carbon nanotubes for nanocomposite structures. Compos Part B. **35**, 95–101 (2004)
7. Li, F., Cheng, H.M., Bai, S., Su, G.: Tensile strength of single-walled carbon nanotubes directly measured from their macroscopic ropes. Appl Phys Lett. **77**, 3161–3163 (2000)
8. Brune, D.A., Bicerano, J.: Micromechanics of nanocomposites: comparison of tensile and compressive elastic moduli, and prediction of effects of incomplete exfoliation and imperfect alignment on modulus. Polymer. **43**, 369–387 (2002)
9. Kwon, H., Estili, M., Takagi, K., Miyazaki, T., Kawasaki, A.: Combination of hot extrusion and spark plasma sintering for producing carbon nanotube reinforced aluminum matrix composites. Carbon. **47**, 570–577 (2009)
10. Peigney, A., Garcia, F.L., Estournès, C., Weibel, A., Laurent, C.: Toughening and hardening in double-walled carbon nanotube/nanostructured magnesia composites. Carbon. **48**, 1952–1960 (2010)
11. Bakshi, S.R., Lahiri, D., Agarwal, A.: Carbon nanotube reinforced metal matrix composites - a review. Int Mater Rev. **55**, 41–64 (2010)
12. Coleman, J.N., Khan, U., Blau, W.J., Gun'ko, Y.K.: Small but strong: a review of the mechanical properties of carbon nanotube–polymer composites. Carbon. **44**, 1624–1652 (2006)
13. Thostenson, E.T., Ren, Z., Chou, T.W.: Advances in the science and technology of carbon nanotubes and their composites: a review. Compos Sci Technol. **61**, 1899–1912 (2001)
14. Schadler, L., Giannaris, S.C., Ajayan, P.M.: Load transfer in carbon nanotube epoxy composites. Appl Phys Lett. **73**, 3842–3844 (1998)
15. Zhu, J., Peng, H., Rodriguez-Macias, F., Margrave, J., Khabashesku, V., Imam, A., Lozano, K., Barrera, E.: Reinforcing epoxy polymer composites through covalent integration of functionalized nanotubes. Adv Funct Mater. **14**, 643–648 (2004)
16. Tarfaoui, M., Lafdi, K., El Moumen, A.: Mechanical properties of carbon nanotubes based polymer composites. Compos Part B: Engineering. **103**, 113–121 (2016)
17. Buryachenko, V.: Micromechanics of Heterogeneous Materials. Springer, New York (2006)
18. Cao, G., Chen, X.: Buckling of single-walled carbon nanotubes upon bending: molecular dynamics simulations and finite element method. Phys Rev B. **73**, 155435 (2006)
19. El Moumen, A., Kanit, T., Imad, A., El Minor, H.: Effect of reinforcement shape on physical properties and representative volume element of particles-reinforced composites: statistical and numerical approaches. Mech Mater. **83**, 1–16 (2015a)
20. Djebara, Y., El Moumen, A., Kanit, T., Madani, S., Imad, A.: Modeling of the effect of particles size, particles distribution and particles number on mechanical properties of polymer-clay nano-composites: numerical homogenization versus experimental results. Compos Part B. **86**, 135–142 (2015)
21. Hashin, Z., Shtrikman, S.: A variational approach to the theory of the elastic behavior of multiphase materials. J Mech Phys Solid. **11**, 127–140 (1963)
22. Mori, T., Tanaka, K.: Average stress in matrix and average elastic energy of materials with misfitting inclusions. Acta Metall. **21**, 571–574 (1973)
23. Christensen, R.M., Lo, K.H.: Solutions for effective shear properties in three phase sphere and cylinder models. J Mech Phys Solid. **27**, 315–330 (1979)
24. Halpin, J.C., Kardos, J.L.: The Halpin-Tsai equations: a review. Polym Eng Sci. **16**, 344–352 (1976)
25. Odegard, G.M., Harik, V.M., Wise, K.E., Gates, T.S.: Constitutive modeling of nanotube-reinforced polymer composite systems. Technical report of NASA CASI, NASA/TM-2001-211044 (2001)
26. Odegard, G., Gates, T., Wise, K.: Constitutive modeling of nanotube reinforced polymer composites. Technical report of American Institute of Aeronautics and Astronautics. AIAA- 2002-1427 (2002a)
27. Odegard, G., Gates, T., Wise, K., Park, C., Siochi, E.: Constitutive Modeling of Nanotube Reinforced Polymer Composites. Technical report, NASA ICASE (2002b)
28. Odegard, G., Gates, T., Wise, K., Park, C., Siochi, E.: Constitutive modeling of nanotube reinforced polymer composites. Compos Sci Technol. **63**, 1671–1687 (2003)

29. Yeh, M.K., Tai, N.H., Liu, J.H.: Mechanical behavior of phenolic-based composites reinforced with multi-walled carbon nanotubes. Carbon. **44**, 1–9 (2006)
30. Hashin, Z., Rosen, W.: The elastic moduli of fiber reinforced materials. J Appl Mech. **31**, 223–232 (1964)
31. Chen, X.L., Liu, Y.J.: Square representative volume elements for evaluating the effective material properties of carbon nanotube-based composites. Comput Mater Sci. **29**, 1–11 (2004)
32. Deng, J., Zhou, Z., Ji, L., Wang, X.: Mechanical behaviour of 3D multi-layer braided composites: experimental, numerical and theoretical study. Appl Compos Mater. (2017). doi:10.1007/s10443-017-9600-1
33. El Moumen, A., Kanit, T., Imad, A., El Minor, H.: Effect of overlapping inclusions on effective elastic properties of composites. Mech Res Commun. **53**, 24–30 (2013)
34. El Moumen, A., Imad, A., Kanit, T., Hilali, E., El Minor, H.: A multiscale approach and microstructure design of the elastic composite behavior reinforced with natural particles. Compos Part B: Engineering. **66**, 247–254 (2014)
35. Ioannou, I., Hodzic, A., Gitman, I.M.: Numerical investigation of thermal and thermo-mechanical effective properties for short fibre reinforced composite. Appl Compos Mater. (2016). doi:10.1007/s10443-016-9569-1
36. Kaddouri, W., El Moumen, A., Kanit, T., Madani, S., Imad, A.: On the effect of inclusion shape on effective thermal conductivity of heterogeneous materials. Mech Mater. **92**, 28–41 (2016)
37. Seidel, G.D., Lagoudas, D.C.: Micromechanical analysis of the effective elastic properties of carbon nanotube reinforced composites. Mech Mater. **38**, 884–907 (2006)
38. Terada, K., Ito, T., Kikuchi, N.: Characterization of the mechanical behaviors of solid-fluid mixture by the homogenization method. Comput Methods Appl Mech Eng. **153**, 223–257 (1998)
39. Pagano, N.J., Yuan, F.G.: The significance of effective modulus theory (homogenization) in composite laminate mechanics. Compos Sci Technol. **60**, 2471–2488 (2000)
40. Manta, A., Gresil, M., Soutis, C.: Predictive model of graphene based polymer nanocomposites: electrical performance. Appl Compos Mater. **24**, 281–300 (2017)
41. Selmi, A., Friebel, C., Doghri, I., & Hassis, H.: Prediction of the elastic properties of single walled carbon nanotube reinforced polymers: a comparative study of several micromechanical models. Compos Sci Technol. **67**(10), 2071–2084 (2007)
42. Fisher, F.T., Bradshaw, R.D., Brinson, L.C.: Effects of nanotube waviness on the modulus of nanotube–reinforced polymers. Appl Phys Lett. **80**, 4647–4649 (2002)
43. Fisher, F.T., Bradshaw, R.D., Brinson, L.C.: Fiber waviness in nanotube–reinforced polymer composites—I: modulus predictions using effective nanotube properties. Compos Sci Technol. **63**, 1689–1703 (2003)
44. Ren, X., Burton, J., Seidel, G.D., Lafdi, K.: Computational multiscale modeling and characterization of piezoresistivity in fuzzy fiber reinforced polymer composites. Int J Solids Struct. **54**, 121–134 (2015)
45. Savvas, D., Stefanou, G., Papadopoulos, V., Papadrakakis, M.: Effect of waviness and orientation of carbon nanotubes on random apparent material properties and RVE size of CNT reinforced composites. Compos Struct. **152**, 870–882 (2016)
46. Gupta, A.K., Harsha, S.P.: Analysis of mechanical properties of carbon nanotube reinforced polymer composites using multi-scale finite element modeling approach. Compos Part B: Engineering. **95**, 172–178 (2016)
47. Choi, J., Shin, H., Cho, M.: A multiscale mechanical model for the effective interphase of SWNT/epoxy nanocomposite. Polymer. **89**, 159–171 (2016)
48. Zhou, H.W., Mishnaevsky, J.R.L., Yi, H.Y., Liu, Y.Q., Hu, X., Warrier, A., Dai, G.M.: Carbon fiber/carbon nanotube reinforced hierarchical composites: effect of CNT distribution on shearing strength. Compos Part B: Engineering. **88**, 201–211 (2016)
49. El Moumen, A., Tarfaoui, M., Hassoon, O., Lafdi, K., Benyahia, H., Nachtane, M.: Experimental study and numerical modelling of low velocity impact on laminated composite reinforced with thin film made of carbon nanotubes. Appl Compos Mater. (2017a). doi:10.1007/s10443-017-9622-8
50. El Moumen, A., Tarfaoui, M., Lafdi, K.: Mechanical characterization of carbon nanotubes based polymer composites using indentation tests. Compos Part B. **114**, 1–7 (2017b)
51. Sherburn, M., Long, A.C.: TexGen open source project open online at http://texgen.sourceforge.net/ (2010)
52. Sherburn, M.: Geometric and mechanical modelling of textiles. PhD thesis. The University of Nottingham, England (2007)
53. Dixit, A., Mali, H.S., Misra, R.K.: Unit cell model of woven fabric textile composite for multiscale analysis. Procedia Eng. **68**, 352–358 (2013)
54. Kanit, T., Forest, S., Galliet, I., Mounoury, V., Jeulin, J.: Determination of the size of the representative volume element for random composites: statistical and numerical approach. Int J Solids Struct. **40**, 3647–3679 (2003)

55. El Moumen, A., Kanit, T., Imad, A., El Minor, H.: Computational thermal conductivity in porous materials using homogenization techniques: numerical and statistical approaches. Comput Mater Sci. **97**, 148–158 (2015b)
56. Daggumati, S., De Baere, I., Van Paepegem, W., Degrieck, J., Xu, J., Lomov, S.V.: Local damage in a 5 – harness satin weave composite under static tension: part I– experimental analysis. Compos Sci Technol. **70**, 1926–1933 (2010)
57. Tarfaoui, M., El Moumen, A., Lafdi, K.: Progressive damage modeling in carbon fibers/carbon nanotubes reinforced polymer composites. Compos Part B. **112**, 185–195 (2017)
58. El Moumen, A., Tarfaoui, M., Lafdi, K., Benyahia, H.: Dynamic properties of carbon nanotubes reinforced carbon fibers/epoxy textile composites under low velocity impact. Compos Part B. **125**, 1–8 (2017c)